Global Journal of Engineering and Technology Advances

eISSN: 2582-5003

Cross Ref DOI: 10.30574/gjeta

Journal homepage: https://gjeta.com/

Global Journal of Engineering and Technology Advances

GJETA

Global Scholar Press, INDIA

(RESEARCH ARTICLE)

Check for updates

Discrepancies between planar and geodesic distances as a function of azimuthal variability

Isaac Ramos Junior [1, *], Leonard Niero da Silveira [1], Vinícius Bergmann Martins [1], Robert Martins da Silva [1], Andréa de Seixas [2], Sílvio Jacks dos Anjos Garnés [2] and Lucas Gonzales Lima Pereira Calado [2]

[1] *Federal University of Pampa, Itaqui Campus, Rio Grande do Sul, Brazil.*

[2] *Department of Cartographic Engineering, Federal University of Pernambuco, Recife, Brazil.*

Global Journal of Engineering and Technology Advances, 2026, 27(03), 139-148

Publication history: Received on 07 May 2026; revised on 14 June 2026; accepted on 17 June 2026

Article DOI: https://doi.org/10.30574/gjeta.2026.27.3.0157

Abstract

Plane surveying measurements usually adopt a topocentric system, suitable for small areas, which can be either a Local Astronomic System - LAS, referenced to the geoid, or a Local Geodetic System - LGS, referenced to the ellipsoid. In modern geodetic measurements, however, a geocentric reference system associated with the ellipsoid is commonly used. Since topocentric systems differ only in the orientation of their axes, the reduction to the ellipsoid and the use of the LGS are important for reconciling field observations and geodetic computations. Nevertheless, planar distances in the LGS do not follow the ellipsoidal surface, requiring conversion. As the radii of the normal sections on the ellipsoid vary with the azimuth, it is hypothesized that the conversion values may also vary. To test this hypothesis, a planar distance of ten thousand meters was used in different azimuths in the LGS with origin at the RSCL station, in the Municipality of Cerro Largo, State of Rio Grande do Sul, Brazil. The resulting differences were on the order of 10^{-5} meters, that, depending on the project objectives, they may be relevant.

Keywords: Local Geodetic System; Normal Section; Topocentric Coordinates; Reference Ellipsoid; Inverse Geodetic Problem

1. Introduction

Traditional surveying measurements are based on a planar reference surface, with Cartesian coordinate axes. This rectangular structure represents the measured points using ordered pairs, usually as north (n) and east (e) or as (x) and (y) and has proven sufficient for surveys of relatively small areas (Van Sickle, 2024).

On the other hand, since the Global Navigation Satellite System - GNSS is associated with the Earth's center of mass, its applications are primarily linked to a Geocentric Cartesian Coordinate System, also referred to, according to Lu, Qu and Qiao (2014, p. 177), as a "Geodesic Cartesian Coordinate System," which is more suitable for global purposes. Such a coordinate system is associated with a mathematical surface, the ellipsoid, used to approximate the shape and size of the Earth (Ogaja, 2024).

Consequently, Geocentric Cartesian Coordinate Systems are not always the most practical choice. In some cases, it is better to adopt a coordinate system with its origin at the observer's location, which lies on the physical surface (Marel, 2020). This type of system is called a Terrestrial Topocentric Coordinate System, or simply a Topocentric System (Vaníček and Krakiwsky, 1986). Traditional terrestrial measurements of distances and angles, using devices such as theodolites and total stations, are tied to this system (Jekeli, 2016). Topocentric Systems are also useful for hybrid positioning that integrate surveys using GNSS with terrestrial measurements (Ogaja, 2024).

* Corresponding author: Isaac Ramos Junior

In this regard, two types of Topocentric Systems can be defined, and they may be two-dimensional or three-dimensional, but are essentially Cartesian (Burkholder, 2001). The system in which the Z or u axis is normal to the equipotential surface at the observation station is called the Local Astronomic System - LAS. The system in which the Z or u axis is normal to the ellipsoidal surface passing through the observation station is called the Local Geodetic System - LGS (Krakiwsky and Wells, 1971). Thus, the only difference between them is the direction of the corresponding axis. This means that the equations for the LGS are obtained simply by replacing the astronomic latitude and longitude with the geodetic latitude and longitude (Jekeli, 2016).

With the use of electronic computational systems, calculations on the ellipsoid have become relatively easy and fast. Therefore, it is convenient to reduce measured angles and long distances to the ellipsoid, analogously to astronomic coordinates. Then, the coordinates obtained by reducing astronomic coordinates to an ellipsoid and by computing the traditional positioning on the ellipsoid can be compared. They should be identical for the same point (Hofmann-Wellenhof and Moritz, 2006). That is, if the proper considerations are made and due care is taken, the LGS is a relevant option among the Topocentric Systems that can be used in relatively small areas.

However, there is a problem common to every LGS. Since they are defined as Cartesian system, long distances may pass through the ellipsoid instead of following its surface, which may seem counterintuitive (Meyer, 2018). In fact, in the case of GNSS, coordinate systems are inherently global and centered at the Earth's center of mass, since the orbits of its satellites are defined with respect to that point. In contrast, terrestrial measurements are fundamentally local and normally expressed in local coordinate systems. Therefore, it is essential to accurately determine the relationships among all the coordinate systems involved (Seeber, 2003).

Even with these points in mind, some specific details can still be listed. One of them is the following: imagine a normal line drawn to the surface of an ellipsoid at a specific point. Now consider a plane that includes this normal line and is therefore perpendicular to the tangent plane to the surface at that point. This plane will intersect the ellipsoid, creating a curve known as a normal section. The radius of curvature of this section varies depending on the azimuth of the intersecting plane (Rapp, 1991).

That is, since the radius of curvature of a normal section passing through any point on the surface of the ellipsoid varies according to the azimuth, and since geodetic distances can be calculated as a function of azimuth by solving the Inverse Geodetic Problem, one may hypothesize that when any planar distance from a point in a given LGS is taken at different azimuths, in the LGS it will obviously remain the same, but it will undergo some change, however slight, when converted to the surface of the ellipsoid, according to the change in azimuth.

For this hypothesis to be analyzed in practical terms, a LGS was established, whose origin point was the RSCL station of the Brazilian Network for Continuous Monitoring of GNSS Systems - RBMC, of the Brazilian Institute of Geography and Statistics - IBGE, located in the Municipality of Cerro Largo, State of Rio Grande do Sul, Brazil. Thus, from the origin, a single planar distance of ten thousand meters was taken at 360 different azimuths, degree by degree, starting at zero, generating 360 points with distinct planar polar coordinates. This distance was chosen because, according to Uren and Price (2010, p. 305), "most engineering projects do not exceed the range of ten to fifteen kilometers in length".

Next, based on planar polar coordinates, planar Cartesian coordinates in the LGS were calculated. From these, geocentric Cartesian coordinates were calculated, which in turn were converted into geodetic coordinates, i.e., into geodetic latitude, geodetic longitude, and geodetic (or ellipsoidal) height. Finally, having obtained the geodetic coordinates, and based on the solution of the Inverse Geodetic Problem, starting from the origin, geodesic distances were determined, one for each azimuth, allowing comparisons in relation to the initial planar distance. All these calculations were performed using scripts written in Python.

A preliminary analysis of azimuth variations was previously presented in Ramos Junior et. al. (2025) for station RSAL. In the present study, the methodology is applied to station RSCL using observations collected approximately one year later, allowing an assessment of the consistency of the observed behavior.

2. Methodology

A Geocentric Cartesian Coordinate System, illustrated in Figure 1, can be defined so that its origin point O is located at the center of the ellipsoid, that is, at the center of the Earth. The Z axis points toward the North Pole, the X axis points toward the point of intersection between the equator and a specific meridian, called the reference meridian, which is usually chosen as the meridian that passes through the Greenwich Observatory, and the Y axis is defined so as to make the system right-handed. Thus, for any point *P*, which in this case is located on the Earth's surface, the Cartesian coordinates become evident (Guo, 2023).

Figure 1 also shows the geodetic coordinates of point *P*. According to Gaspar (2008, p. 93), "geodetic coordinates, defined on a reference ellipsoid, are geodetic latitude, geodetic longitude, and geodetic (or ellipsoidal) height". Thus, for a given ellipsoid, geodetic latitude (ϕ), geodetic longitude (λ), and ellipsoidal height (h) are the geodetic coordinates of *P* (Jekeli, 2016). The geodetic latitude of a point is the angle between the normal to the ellipsoid passing through that point and the equatorial plane; the geodetic longitude of a point is the angular distance between the plane containing the Greenwich meridian and the plane containing the meridian of that point, measured in the equatorial plane, with positive direction toward the east; and the ellipsoidal height of a point is the linear distance, measured from the surface of the ellipsoid, along the normal, to the point (Krakiwsky e Wells, 1971).

Also in Figure 1, an LGS can be seen, with its origin at point *P*, located in the central region of interest, on the physical surface of the Earth, where the observer is situated. Thus, the origin of the LGS is topocentric rather than geocentric (Meyer, 2018). This system can be defined as follows (Soler e Hothem, 1988):

- Origin at a point *P* on the physical surface, with known geocentric Cartesian coordinates (X_0, Y_0, Z_0) and known geodetic coordinates (ϕ_0, λ_0, h_0)
- The *u* axis coincides with the normal to the ellipsoid passing through *P*, positive toward the geodesic zenith
- The *e* axis is perpendicular to the *u* axis and to the plane of the meridian section passing through *P*, positive toward the East
- The *n* axis is perpendicular to the *e* axis and to the *u* axis, forming a right-handed system, positive toward to the North

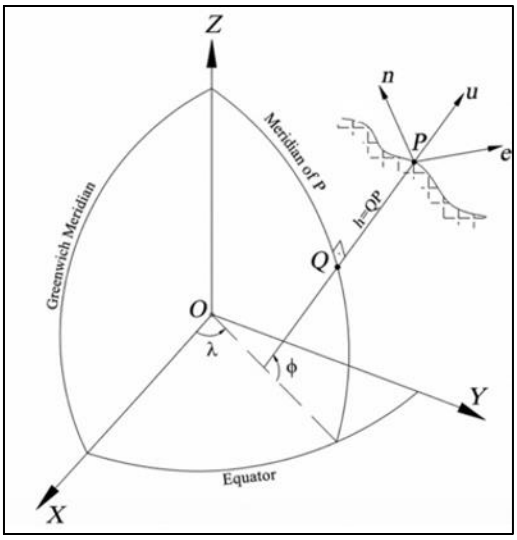

Figure 1 Geocentric Cartesian (*X, Y, Z*), Geodetic ($\boldsymbol{\phi}, \boldsymbol{\lambda}, \boldsymbol{h}$) and LGS (*e, n, u*) Coordinates

Thus, the LGS, with its coordinate system (*e, n, u*), is similar to the Geocentric Cartesian Coordinate System (*X, Y, Z*). Both are Cartesian, that is, both have three mutually perpendicular axes. The axes have the same scale, and the coordinates are composed of the distances from their respective origins along the coordinate axes. In fact, any coordinate system (*e, n, u*) is simply a Geocentric Cartesian Coordinate System translated from its origin to the local origin and then rotated so that the axes align with the local cardinal directions (Meyer, 2018).

This means that, from the rotation and translation of a Geocentric Cartesian Coordinate System that has points with known coordinates (*X, Y, Z*), it is possible to obtain an LGS with coordinates (*e, n, u*) for those same points, with origin at a point *P*, generally located at the center of the area of interest. To perform the conversion calculations, equation (1) can be used, according to (Soler and Hothem, 1988):

$$\begin{bmatrix} e \\ n \\ u \end{bmatrix} = \begin{bmatrix} -sin\lambda_0 & cos\lambda_0 & 0 \\ -sin\phi_0 cos\lambda_0 & -sin\phi_0 sin\lambda_0 & cos\phi_0 \\ cos\phi_0 cos\lambda_0 & cos\phi_0 sin\lambda_0 & sin\phi_0 \end{bmatrix} \begin{bmatrix} X - X_0 \\ Y - Y_0 \\ Z - Z_0 \end{bmatrix} \tag{1}$$

Equation (1) presents the final form for converting geocentric Cartesian coordinates (*X, Y, Z*) into local Cartesian coordinates (*e, n, u*) in the LGS. In an optional step, shifts along the axes may be added as a convenience to make all coordinates within the project area positive (Wolf, Dewitt and Wilkinson, 2014). In this study, however, no such shifts were introduced, since they do not affect the results and the objective was not to determine the coordinates themselves, but rather to compare planar and ellipsoidal distances as a function of azimuthal variation.

Thus, the coordinates (e_0, n_0, u_0) for the RSCL station, the origin of the LGS, were established as shown in Table 1, which also presents its geocentric Cartesian coordinates, as officially published by IBGE (2026).

Table 1 Geocentric Cartesian coordinates and LGS Coordinates of the RSCL Station, in SIRGAS2000

Station	X_0 (m)	Y_0 (m)	Z_0 (m)	e_0 (m)	n_0 (m)	u_0 (m)
RSCL	3.248.119,5811	-4.596.792,9901	-2.990.511,4333	0,000	0,000	0,000

With the geocentric cartesian coordinates of the origin in hand, the first step was to convert them into geodetic coordinates. This procedure was carried out according to equations (2) to (9), following (Hofmann-Wellenhof and Moritz, 2006):

$$\lambda = atan(\frac{Y}{X}) \tag{2}$$

$$p = \sqrt{X^2 + Y^2} \tag{3}$$

$$\theta = atan(\frac{Za}{pb}) \tag{4}$$

$$e'^2 = \frac{a^2 - b^2}{b^2} \tag{5}$$

$$e^2 = \frac{a^2 - b^2}{a^2} \tag{6}$$

$$\phi = atan(\frac{Z + e'^2 b(sin^3\theta)}{p - e^2 a(cos^2\theta)}) \tag{7}$$

$$N = \frac{a^2}{\sqrt{a^2cos^2\phi + b^2sin^2\phi}} \tag{8}$$

$$h = \frac{p}{cos\phi} - N \tag{9}$$

In equations (4) to (9), the values for the semi-major axis and the semi-minor axis, both related to the GRS-80 ellipsoid, are, respectively, a = 6,378,137.0000 meters and b = 6,356,752.3141 meters, according to Moritz (2000).

After these calculations, the next stage began with the topocentric coordinates of the origin, with a distance in the *en* plane of the LGS chosen as ten thousand meters, and with 360 planar azimuths in the LGS, selected one degree at a time, with values from 0° to 359°. These data constituted a set of 360 points with known planar polar coordinates in the LGS. Thus, after obtaining the planar polar coordinates in the LGS for the points of interest, the next stage consisted of converting them into Cartesian coordinates in the *en* plane of the LGS.

With the coordinates of the points calculated in the *en* plane of the LGS, in order to make the conversion to geocentric Cartesian coordinates possible, equation (1) was manipulated so that the coordinates (*X, Y, Z*) were made explicit. Thus, this manipulation can be seen in equations (10) to (12).

$$\begin{bmatrix} -sin\lambda_0 & cos\lambda_0 & 0 \\ -sin\phi_0 cos\lambda_0 & -sin\phi_0 sin\lambda_0 & cos\phi_0 \\ cos\phi_0 cos\lambda_0 & cos\phi_0 sin\lambda_0 & sin\phi_0 \end{bmatrix}^{-1} \begin{bmatrix} e \\ n \\ u \end{bmatrix} = \begin{bmatrix} X - X_0 \\ Y - Y_0 \\ Z - Z_0 \end{bmatrix} \tag{10}$$

$$\begin{bmatrix} X - X_0 \\ Y - Y_0 \\ Z - Z_0 \end{bmatrix} = \begin{bmatrix} -sin\lambda_0 & cos\lambda_0 & 0 \\ -sin\phi_0 cos\lambda_0 & -sin\phi_0 sin\lambda_0 & cos\phi_0 \\ cos\phi_0 cos\lambda_0 & cos\phi_0 sin\lambda_0 & sin\phi_0 \end{bmatrix}^{-1} \begin{bmatrix} e \\ n \\ u \end{bmatrix} \tag{11}$$

$$\begin{bmatrix} X \\ Y \\ Z \end{bmatrix} = \begin{bmatrix} -sin\lambda_0 & cos\lambda_0 & 0 \\ -sin\phi_0 cos\lambda_0 & -sin\phi_0 sin\lambda_0 & cos\phi_0 \\ cos\phi_0 cos\lambda_0 & cos\phi_0 sin\lambda_0 & sin\phi_0 \end{bmatrix}^{-1} \begin{bmatrix} e \\ n \\ u \end{bmatrix} + \begin{bmatrix} X_0 \\ Y_0 \\ Z_0 \end{bmatrix} \tag{12}$$

The next step was to carry out the conversion calculations from geocentric Cartesian coordinates (*X, Y, Z*) to geodetic coordinates (ϕ, λ, h) but this time for the points of interest, based on equations (2) to (9).

With the geodetic coordinates of the points, it was possible to calculate the geodesic distances between the origin of the LGS, which already had known coordinates, and each of these points. This step was carried out by solving the Inverse Geodetic Problem. This is a classic problem in which, from the geodetic latitudes and longitudes of two points, the geodesic distance, the geodesic azimuth and the reverse geodesic azimuth between them are determined (Sjöberg and Shirazian, 2012). In geodesy, the geodesic line, or simply geodesic, is understood as the shortest path between two points on the surface of the ellipsoid, and the length of this line is called the geodesic distance (Gaspar, 2008).

A possible solution to this problem, which was chosen in this article, can be found in Vincenty (1975). However, since it is an iterative procedure, the sequence of calculations will be presented for any two points with coordinates (ϕ_1, λ_1) and (ϕ_2, λ_2).

Thus, initially, the reduced latitudes U1 and U2 were calculated for the points, according to equations (13) and (14) (Vincenty, 1975):

$$U_1 = atan((1 - f)tan\phi_1) \tag{13}$$

$$U_2 = atan((1 - f)tan\phi_2) \tag{14}$$

In equations (13) and (14), *f* = 0.00335281068118 was used, which is the flattening of the GRS-80 ellipsoid, according to Moritz (2000).

The next step was to calculate the difference between the geodetic longitudes, here called *L*. However, at first, it was set equal to the difference between the longitudes on an auxiliary sphere, here denoted by λ_a, according to equation (15):

$$\lambda_a = L = \lambda_2 - \lambda_1 \tag{15}$$

Due to the consideration made in equation (15), it was possible to begin an iterative process until the convergence of λ_a, according to equations (16) to (21) (Vincenty, 1975):

$$sin\sigma = \sqrt{(cosU_2 sin\lambda_a)^2 + (cosU_1 sinU_2 - sinU_1 cosU_2 cos\lambda_a)^2} \tag{16}$$

$$cos\sigma = sinU_1 sinU_2 + cosU_1 cosU_2 cos\lambda_a \tag{17}$$

$$\sigma = atan(\frac{sin\sigma}{cos\sigma}) \tag{18}$$

$$sin\alpha = \frac{cosU_1 cosU_2 sin\lambda_a}{sin\sigma} \tag{19}$$

$$cos^2\alpha = 1 - sin^2\alpha \tag{20}$$

$$cos2\sigma_m = cos\sigma - \frac{2sinU_1 sinU_2}{cos^2\alpha} \tag{21}$$

In equations (16) to (21), σ is the angular distance between the two points on the sphere; σ_m is the angular distance on the sphere measured from the equator to the midpoint of the geodesic line; and α is the azimuth of the geodesic line at the Equator.

Equation (21) includes an observation. In it, if $\cos^2\alpha = 0$, then $\cos 2\sigma_m = 0$, and the iteration proceeds normally. Thus, the calculations continued according to equations (22) and (23) (Vincenty, 1975):

$$C = \frac{f}{16} cos^2\alpha[4 + f(4 - 3cos^2\alpha)] \tag{22}$$

$$\lambda_{novo} = L + (1 + C) f sin\alpha(\sigma + C sin\sigma(cos2\sigma_m + C cos\sigma(1 - 2cos^2 2\sigma_m))) \tag{23}$$

With λ_{novo} in hand, it was verified whether the absolute value of the subtraction between it and λ_a was smaller than a value ϵ prescribed for convergence. According to Vincenty (1975, p. 90), "the iteration procedure must be continued until the change in the value of λ_a is negligible." In this article, $\epsilon = 10^{-12}$ was used as the convergence value. Thus, as long as this value was not reached, the calculations were repeated, always using the last λ_{novo} until the objective was achieved.

After convergence was resolved, the calculations continued by means of equations (24) to (27), according to Vincenty (1975):

$$u^2 = cos^2\alpha(\frac{a^2 - b^2}{b^2}) \tag{24}$$

$$A = 1 + \frac{u^2}{16384}(4096 + u^2(-768 + u^2(320 - 175u^2))) \tag{25}$$

$$B = \frac{u^2}{1024}(256 + u^2(-128 + u^2(74 - 47u^2))) \tag{26}$$

$$\Delta\sigma = B sin\sigma(cos2\sigma_m + \frac{B}{4}(cos\sigma(-1 + 2cos^2 2\sigma_m) - \frac{B}{6} cos2\sigma_m(-3 + 4sin^2\sigma)(-3 + 4cos^2 2\sigma_m))) \tag{27}$$

At this point, the geodesic distance s and the geodesic azimuths α_1 and α_2 of the reciprocal normal sections could then be calculated according to equations (28) to (30), following Vincenty (1975):

$$s = bA(\sigma - \Delta\sigma) \tag{28}$$

$$\alpha_1 = atan(\frac{cosU_2 sin\lambda}{cosU_1 sinU_2 - sinU_1 cosU_2 cos\lambda}) \tag{29}$$

$$\alpha_2 = atan(\frac{cosU_1 sin\lambda}{-sinU_1 cosU_2 + cosU_1 sinU_2 cos\lambda}) \quad (30)$$

After the calculations, the geodesic distances and geodesic azimuths obtained were validated using the online geodetic calculator available from Australian Government (2026). Finally, the comparisons and the statistical analyses in relation to the initial distance of ten thousand meters in the *en* plane of the LGS became possible.

3. Results and discussions

The first set of results consists of the geodetic coordinates of the RSCL origin station, computed from its geocentric Cartesian coordinates, as shown in Table 2.

Table 2 Geodetic coordinates of RSCL Station, in SIRGAS2000

Station	ϕ_0	λ_0	h (m)
RSCL	-28º 08' 30,76928"	-54º 45' 17,13341"	280,904

The second set of results obtained concerned the conversion of planar polar coordinates into local Cartesian coordinates (*e,n,u*) for the 360 points. For better understanding, Figure 2 shows the plot of the results for the coordinates in the *en* plane, confirming that the 10,000 meters and the azimuths correspond to the coordinates. Evidently, after the calculations, the coordinates related to the *u* component resulted in zero for all points.

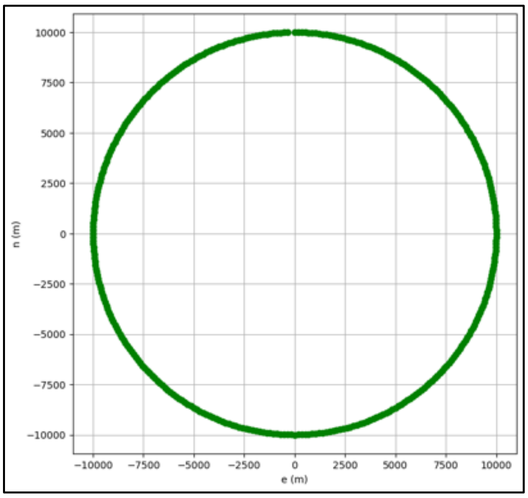

Figure 2 Visualization of the results for the coordinates of all 360 points in the *en* plane

Subsequently, the geocentric Cartesian coordinates (*X, Y, Z*) were computed for all points, according to Equation (12). It should be noted that the values of the *Z* component are not zero, since, in a geocentric Cartesian geodetic system, the *Z* component of a point is zero only if it lies on the equatorial plane. After this stage, the geodetic latitudes and longitudes were calculated for each of the points.

At this stage, it was possible to compute the geodesic distances using Vincenty's equations for the Inverse Geodetic Problem. This step was carried out, and the geodesic distances were calculated for each of the points, taking RSCL as the origin. After the calculations, the results were plotted in a graph so that they could be analyzed (Figure 3).

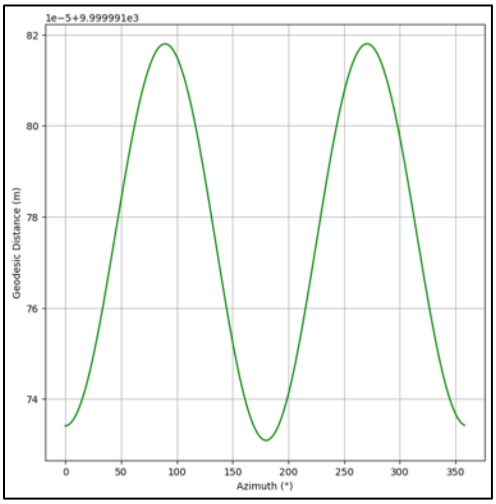

Figure 3 Geodesic distances according to azimuth variation

It should be noted that, in Figure 3, because the results are highly peculiar, the values on the ordinate axis are displayed with a scale of $1e^{-5} + 9.999991e^{3}$, indicating that the values shown on this axis must be interpreted by adding this scale. Thus, for example, when reading the value 78 on this axis, it means that the ellipsoidal distance is $78 \times 10^{-5} + 9.999991 \times 10^{3}$ m, or 9,999.99178 m.

Figure 3 also shows homogeneity in the results, mainly because the geodesic distances symmetrically follow the variations in azimuth. Thus, for example, the largest values occur at azimuths of 90° and 270°, whereas the smallest values occur at azimuths of 0° and 180°, and these are also respectively equal. Table 3 presents these values, in addition to the mean, median, and standard deviation.

Table 3 Basic statistics of the results for the geodesic distances

Mean (m)	Median (m)	Standard Deviation (m)	Minimum (m)	Maximum (m)
9,999.991775391	9,999.991775679	0.000030207	9,999.991730888	9,999.991818001

Table 3 shows that the mean and the median have virtually the same value, indicating a symmetric distribution. In addition, since the standard deviation has a very low value, this shows that the variability of the results is extremely low, being concentrated around the mean.

Once the results for the geodesic distances had been obtained and analyzed, the calculations and analyses concerning the differences between the distance of 10,000 meters in the *en* plane and the geodesic distances found were carried out. These differences can be visualized in Figure 4.

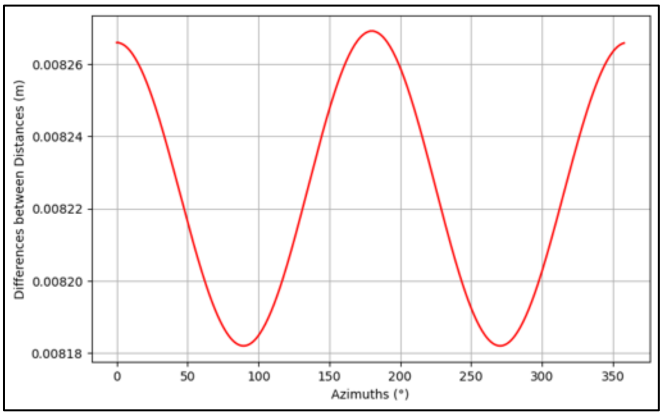

Figure 4 Differences between the reference distance in the *en* plane and the geodesic distances

Figure 4 shows the homogeneity of the results, mainly because the differences between the distances symmetrically follow the changes in azimuth. Thus, for example, the smallest values for the differences between the distances occur at azimuths of 90° and 270° and are equal, whereas the largest values for the differences between the distances occur at azimuths of 0° and 180°, which are also equal. These results are presented in Table 4 and corroborate those in Figure 4, since the largest values are closer to ten thousand meters, which leads to the smallest differences between the compared distances.

Table 4 also presents the results for the mean, median, and standard deviation regarding the differences between the distances. Thus, analogously to what occurred with the geodesic distances, it was found that the mean and the median in this case also have practically the same value, indicating a symmetric distribution, and that, since the standard deviation has a very low value, this shows that the variability of the results is extremely low, being concentrated around the mean.

Table 4 Basic statistics of the results for the differences between the distances

Mean (m)	Median (m)	Standard Deviation (m)	Minimum (m)	Maximum (m)
0,008224608	0,0082243209	0,0000302072	0,00818199	0,008269111

4. Conclusion

This article investigated the differences between a planar distance of ten thousand meters in an LGS with origin at the RSCL station of the RBMC, taken at 360 different azimuths, in relation to the geodesic distances converted from this configuration. Thus, the calculations for the geodesic distances were carried out, and an initial homogeneity was observed in the results, mainly because the geodesic distances symmetrically follow the changes in azimuth. As shown in Figure 3 and Table 3, the largest values for the geodesic distances occurred at azimuths of 90° and 270°, whereas the smallest values occurred at azimuths of 0° and 180°. These differences are in the order of 10^{-5} m.

Regarding the differences between the reference planar distance and the geodesic distances, the same homogeneity was found in the results. In addition, as shown in Figure 4 and Table 4, the smallest values for the differences between the distances occurred at azimuths of 90° and 270°, whereas the largest values occurred at azimuths of 0° and 180°. These results corroborate the geodesic distance results, since their largest values are closer to ten thousand meters, leading to the smallest differences. Therefore, it was observed that there are differences among geodesic distances measured from a point when the azimuth varies. Consequently, because this does not occur with a planar distance in an LGS, it was verified that there are differences between the two types of distance when only the azimuth changes. For a planar distance of ten thousand meters, such differences are small, in the order of 10^{-5} m; however, depending on the project objectives, they may be relevant.

Compliance with ethical standards

Disclosure of conflict of interest

No conflict of interest to be disclosed.

References

[1] Australian Government. *Geodetic calculators - Vincent inverse*. Commonwealth of Australia, Canberra: Geoscience Australia, 20 May. 2026. Available at: https://geodesyapps.ga.gov.au/vincenty-inverse. Accessed: 20/05/2026.

[2] Burkholder E. *Designing a local coordinate system*. New Mexico state university. Las cruces, 2001.

[3] Gaspar J. *Dicionário de ciências cartográficas*. Lisboa: Lidel edições técnicas, 2008. ISBN 9789727575466

[4] Guo J. *Physical geodesy, a theoretical introduction*. Springer textbooks in earth sciences, geography and environment. Springer Nature Switzerland. Cham: 2023. https://doi.org/10.1007/978-3-031-23320-3

[5] Hofmann-Wellenhof B, Moritz H. *Physical geodesy*. Wien: Springer-Verlag, 2006. https://doi.org/10.1007/978-3-211-33545-1

[6] Instituto Brasileiro de Geografia e Estatística – IBGE. *Relatório de informação da estação RSCL - Cerro Largo*. Rio de janeiro: IBGE, 25 mai. 2026. Available at: https://geoftp.ibge.gov.br/informacoes_sobre_posicionamento_geodesico/rbmc/relatorio/descritivo_rscl.pdf. Accessed: 25/05/2026.

[7] Jekeli C. *Geometric reference systems in geodesy*. Division of Geodetic Science, Ohio State University. Columbus: 2016.

[8] Krakiwsky E, Wells D. *Coordinate systems in geodesy*. Lecture notes n° 16. University of New Brunswick. Fredericton: 1971.

[9] Lu Z, Qu Y, Qiao S. *Geodesy*. Springer-Verlag. Heidelberg, 2014. https://doi.org/10.1007/978-3-642-41245-5

[10] Marel H. *Lecture notes on reference systems for surveying and mapping*. Delft university of technology. Delft: 2020.

[11] Meyer T. *Introduction to geometrical and physical geodesy*. Redlands: Esri press, 2018. ISBN 1589485327, 9781589485327

[12] Moritz H. Geodetic reference system 1980. *Journal of geodesy*, 74, p. 128–133, 2000. https://doi.org/10.1007/s001900050278

[13] Ogaja C. *An introduction to GNSS geodesy and applications*. Second edition. Cham: Springer Nature Switzerland, 2024. https://doi.org/10.1007/978-3-031-74494-5

[14] Ramos Junior I, Silveira L, Seixas A, Garnés S, Calado L. Discrepâncias entre distâncias planas e geodésicas em função da variabilidade azimutal. Annals of I Congresso Internacional de Regularização Fundiária & VIII Simpósio Brasileiro de Ciências Geodésicas e Tecnologias da Geoinformação, Recife, PE, Brazil, 23-25 September 2025. https://doi.org/10.5281/zenodo.17153840

[15] Rapp R. *Geometric geodesy, part I*. The Ohio State University. Columbus: 1991.

[16] Seeber G. *Satellite geodesy, 2nd completely revised and extended edition*. New York: Walter de Gruyter, 2003. ISBN-10 : 3110175495

[17] Sjöberg L, Shirazian M. Solving the direct and inverse geodetic problems on the ellipsoid by numerical integration. *Journal of surveying engineering*. Volume 138, issue 1, p. 09-16, 2012. https://doi.org/10.1061/(ASCE)SU.1943-5428.0000061

[18] Soler T, Hothem L. Coordinate systems used in geodesy: basic definitions and concepts. *Journal of surveying engineering*. Volume 114, issue 2, p. 84-97, 1988. https://doi.org/10.1061/(ASCE)0733-9453(1988)114:2(84)

[19] Van Sickle J. *GPS and GNSS for land surveyors*. Fifth edition. Boca Raton: CRC press, 2024. https://doi.org/10.1201/9781003405238

[20] Vaníček P, Krakiwsky E. *Geodesy: the concepts*. Second edition. Amsterdam: Elsevier science, 1986. ISBN 1483290794, 9781483290799

[21] Vincenty T. Direct and inverse solutions of geodesics on the ellipsoid with application of nested equations. *Survey review*, XXII, 176, p. 88-93, April 1975. https://doi.org/10.1179/sre.1975.23.176.88

[22] Wolf P, Dewitt B, Wilkinson B. *Elements of photogrammetry with applications in GIS, fourth edition*. New York: McGraw-Hill education, 2014. ISBN 9780071761123